

# SIGNAL PROCESSING CRITERIA FOR SINGLE HYDROPHONE SOUND SOURCE RANGING IN SHALLOW WATERS

Sung-Hoon Byun      Korea Research Institute of Ships and Ocean engineering (KRISO),  
University of Science and Technology (UST)  
Jeong-Bin Jang      Korea Research Institute of Ships and Ocean engineering (KRISO),  
University of Science and Technology (UST)

## 1 INTRODUCTION

It is common to use a hydrophone sensor array to localize underwater sound sources. However, its performance being dependent on the number of sensor elements, sufficient array dimension is required to guarantee the localization performance, which makes handling the array difficult and place the burden of processing large amounts of data. As an alternative to the array processing, a single-hydrophone source localization based on various waveguide effects have been studied<sup>1,2,3,4,5</sup>.

In particular, the field differencing<sup>1</sup> of a single hydrophone signal has the advantage of being simple to calculate and being able to use various types of sound sources. Basically, the field differencing method correlates the received pressure fields at different ranges from a radiating source, and the resulting cross-correlation field has an oscillation pattern providing clues about the radial velocity of moving sound source. Accordingly, the estimated radial velocity can be used to calculate the range from the receiver via fitting with the closest point approach (CPA) velocity model if the CPA is observed or from the waveguide invariant if it is not observed. Its effectiveness was proven using shallow water environmental experiment data<sup>1,4</sup> and was also proven even for the reliable acoustic path (RAP) experiment data<sup>3</sup> where the receiver depth was 4500m. Recently, its application has been extended to tracking underwater unmanned vehicle<sup>2</sup>.

Although the field differencing method is quite simple, it has been observed that errors can occur in the velocity estimation, and performance can deteriorate depending on the parameter values used in the signal processing. With respect to it, this study reviews the signal processing parameters used in the field differencing method and their underlying constraints which needs to be considered during its application. We focus on the velocity estimation problem since the range calculation can be regarded as a subsidiary procedure of velocity estimation if the environmental information such as sound speed profile and waveguide invariant are known accurately enough.

## 2 SOURCE VELOCITY ESTIMATION BY THE FIELD DIFFERENCING METHOD

The field differencing method<sup>1</sup> uses the cross-correlation field  $I_c(R, \Delta r)$  which is defined as

$$I_c(R, \Delta r) = \Re[p(R - \Delta r/2)p^*(R + \Delta r/2)], \quad (1)$$

where  $R$  is the average range of the source, and  $\Delta r$  is the range interval between the cross correlated signals when the source is at  $R$ .  $\Re[\cdot]$  denotes the real part of a complex value. When the source moves with the radial velocity  $v_r$ , the cross-correlation field can be shown to have the following relation according to the normal mode theory<sup>1,6</sup>,

$$I_c(R, \Delta r) \propto \cos(\bar{k}_r \Delta r) = \cos\left(\frac{2\pi f}{\bar{v}_p} v_r \Delta t\right), \quad (2)$$

where  $\bar{k}_r$  is the average wave number of modes,  $f$  is the signal frequency, and  $\bar{v}_p$  is the average modal phase speed, i.e.  $\bar{k}_r = 2\pi f / \bar{v}_p$ .

It is observed that Eq.(2) will have the maxima when  $\bar{k}_r \Delta r$  is an integral multiple of  $2\pi$ . Both the broadband and the narrowband signal can be used to estimate  $v_r$  from Eq.(2). For narrowband case, we can vary the time interval  $\Delta t$  with  $f$  fixed, whereas for broadband case, we can vary the frequency  $f$  with  $\Delta t$  fixed to find the remaining factors including  $v_r$ . The radial source velocity  $v_r$  can be estimated by the Fourier transform of  $I_c(R, \Delta r)$ . That is,  $I_c(R, 0), I_c(R, \Delta t), \dots, I_c(R, (N-1)\Delta t)$  are Fourier transformed to estimate  $v_r$  at each range  $R$ . The peak position in the normalized abscissa of the transform domain contains the velocity information. In particular, if the peak position of the Fourier transform for the narrowband case is denoted as  $p$ , then  $v_r$  is obtained by

$$v_r = \frac{p}{f} \frac{\bar{v}_p}{\Delta t}. \quad (3)$$

Here,  $\bar{v}_p$  can be approximated by the average sound speed in the waveguide, and  $f$  is the signal frequency in  $Hz$ .

### 3 SIGNAL PROCESSING PARAMETERS OF THE FIELD DIFFERENCING METHOD

In this section, we review the signal processing parameters for calculating the cross correlation field and discuss their impact on the velocity estimation. The SWellEX-96 experiment data<sup>7</sup> was used for analyzing the effects of parameters. In particular, we used the VLA data of the event S5 which was from a source towed at a 54 m depth and at a constant speed of 2.5 m/s along a linear track as described in Figure 1. The data from the element no.13 at the depth of 189.8 m was used among twenty one elements available for the VLA. As shown in the figure, the track has the CPA point to the VLA after about three quarters of total track length.

We discuss only the narrowband case in the below. However, because the frequency  $f$  and the time interval  $\Delta t$  are reciprocal in Eq.(2), the constraints can be inferred similarly for the broadband case.

**Correlation time interval ( $\Delta t$ )** Correlation time interval  $\Delta t$  controls the time lag between two signals correlated in Eq.(1) where  $\Delta r = v_r \Delta t$ . When  $I_c$  is Fourier transformed to estimate the velocity,  $\Delta t$  plays the role of sample period. Thus, it determines the maximum radial source velocity according to the sampling theorem. Figure 2 shows the results for different time intervals, where the case (b)  $\Delta t = 1.0s$  exceeds the allowed sample period for the given source velocity. Using such a long time interval results in velocity aliasing, as shown in Figure 1(b).

The relationship between the maximum radial velocity and the time interval is as follows:

$$v_{r,max} = \frac{1}{2} \frac{\bar{v}_p}{f \Delta t}. \quad (4)$$

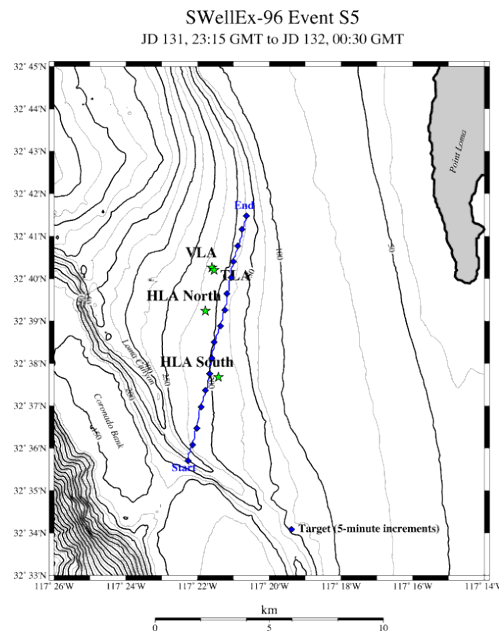


**Figure 1: Map of the ship trajectory of the event S5 in the SWellEX-96 experiment.**

Another constraint on  $\Delta t$  for the narrowband case is that it must be an integral multiple of signal period. This is because if the time interval is not a multiple of the cycle, the pressure field used for cross-correlation are phase shifted relative to each other, and such phase shift causes an velocity offset<sup>8</sup>. Figure 3(a) shows the case when  $\Delta t$  is an integral multiple of signal period ( $1=1/49 \times 49$ ), and Figure 3(b) shows the case when it is not ( $0.4906 \approx 1/49 \times 24.04$ ). Due to the phase offset, the source velocity is offset from the true value which was denoted by the dashed line in the figure.

**Window length ( $L$ )** Window length  $L$  is the length of the short-time Fourier transform which is used to acquire the pressure field of the target frequency. The effect of window length depends on the frequency of the signal. For low frequencies, a longer window length helps reducing the variance of the estimation results, whereas degrading the performance for high frequencies. Figure 4 shows the estimated velocity using different window lengths for both low (166  $Hz$ ) and high (388  $Hz$ ) frequency signals. At high frequency case, increased window length results in poor velocity estimation particularly for the time between 0 and 2000 seconds, while there is no noticeable change for low frequency case.

Figure 5 shows the average value of the estimated velocity in the period between 0 and 2400 seconds. During the period, the source is quite distant to the receiver, so the observed radial velocity should be appear almost constant. However, in Figure 5, the estimated value deviates from the known source speed at the high frequency cases, i.e. 338 and 388  $Hz$ . For those frequencies, the average speed decreases to less than the known sound source speed, and this is due to the influence of the period where the velocity is not estimated properly, as shown in Figure 4(d) and (f).

**FFT length ( $N$ )** The FFT length  $N$  represents the size of  $I_c$  which is Fourier transformed to calculate the source velocity. According to the time-frequency relationship of the Fourier transform, as  $N$  increases, the velocity resolution improves, but the time resolution may deteriorate. This fact can be confirmed in Figure 6, which shows a comparison of different FFT lengths. When  $N$  is long, i.e.  $N=300$ , we can see that the velocity resolution improves as expected, but the resolution on the time axis deteriorates, as observed

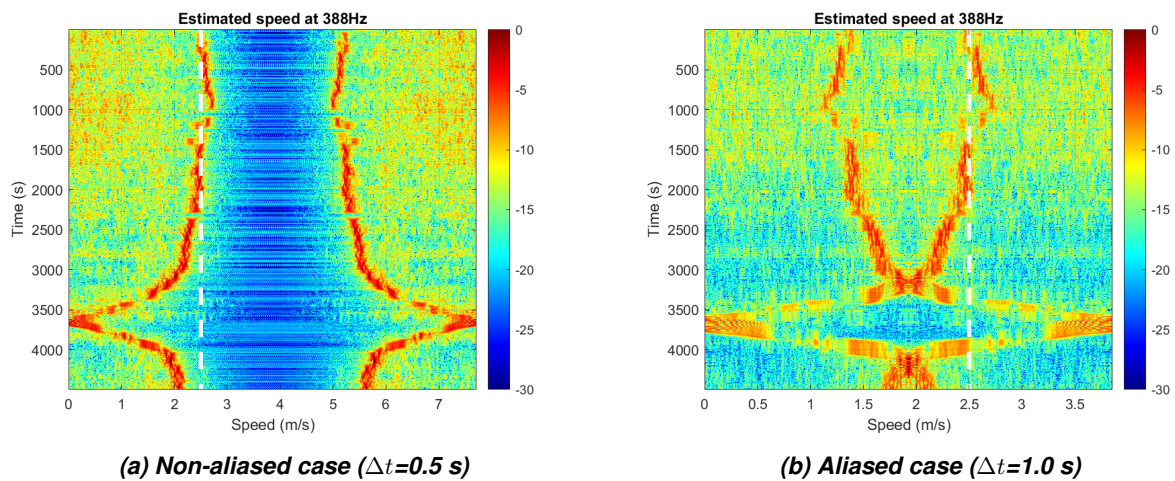


**Figure 2: The sampling theorem criterion for  $\Delta t$ .**

especially near the CPA.

## 4 CONCLUSION

This study analyzed the signal processing parameters of the field differencing method for estimating the source velocity (range) using a single hydrophone. In order to prevent the method from producing incorrect results, it is important to properly understand the role and constraints of its processing parameters. Using the SWellEX-96 experimental data, constraints and performance trade-offs of the processing parameters were exemplified and interpreted.

## ACKNOWLEDGMENTS

This work was supported by Korea Research Institute for defense Technology planning and advancement(KRIT) - Grand funded by the Korea government(DAPA(Defense Acquisition Program Administration))(No. KRIT-CT-23-026, Integrated Underwater Surveillance Research Center for Adapting Future Technologies, 2023)

## REFERENCES

1. Rakotonarivo, S. T. and Kuperman, W. A. (2012). Model-independent range localization of a moving source in shallow water. The Journal of the Acoustical Society of America, 132(4), 2218–2223. <https://doi.org/10.1121/1.4748795>
2. Jang, Junsu, and Florian Meyer. “Navigation in Shallow Water Using Passive Acoustic Ranging,” no. MI (2023). <http://arxiv.org/abs/2306.06426>.
3. Yang, K.-D., Li, H., Duan, R. and Yang, Q.-L. (2017). Analysis on the Characteristic of Cross-Correlated Field and Its Potential Application on Source Localization in Deep Water. Journal of Computational Acoustics, 25(02), 1750001. <https://doi.org/10.1142/S0218396X17500011>
4. Cockrell, Kevin L., and Henrik Schmidt. “Robust Passive Range Estimation Using the Waveg-

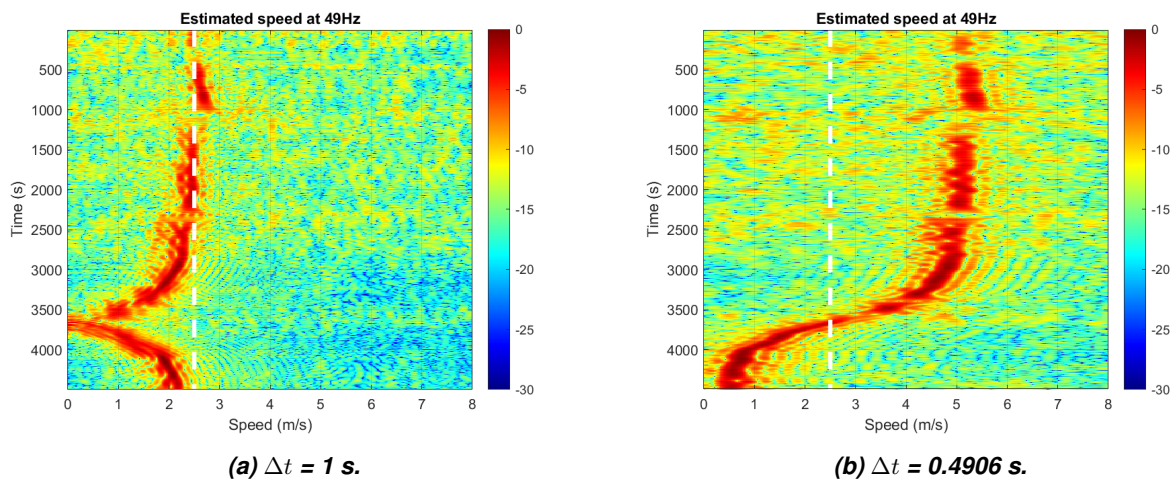


**Figure 3: Effect of relationship between the time interval ( $\Delta t$ ) and the signal period ( $1/f$ ).**

- uide Invariant." The Journal of the Acoustical Society of America 127, no. 5 (2010): 2780–89. <https://doi.org/10.1121/1.3337223>.
5. Young, Andrew H, H Andrew Harms, Granger W Hickman, Jeffrey S Rogers, and Jeffrey L Krolik. "Waveguide-Invariant-Based Ranging and Receiver Localization Using Tonal Sources of Opportunity." IEEE Journal of Oceanic Engineering 45, no. 2 (2020): 631–44. <https://doi.org/10.1109/JOE.2018.2883855>.
6. Jensen, F B, W A Kuperman, M B Porter, and H Schmidt. Computational Ocean Acoustics. Modern Acoustics and Signal Processing. Springer New York, 2011.
7. <http://swellex96.ucsd.edu/>
8. Wang, C., Wang, J., and Du, P. (2017). Estimation of moving target speed using weak line spectrum of single-hydrophon. 2017 IEEE International Conference on Signal Processing, Communications and Computing, ICSPCC 2017, 2017-Janua, 1–5. <https://doi.org/10.1109/ICSPCC.2017.8242462>



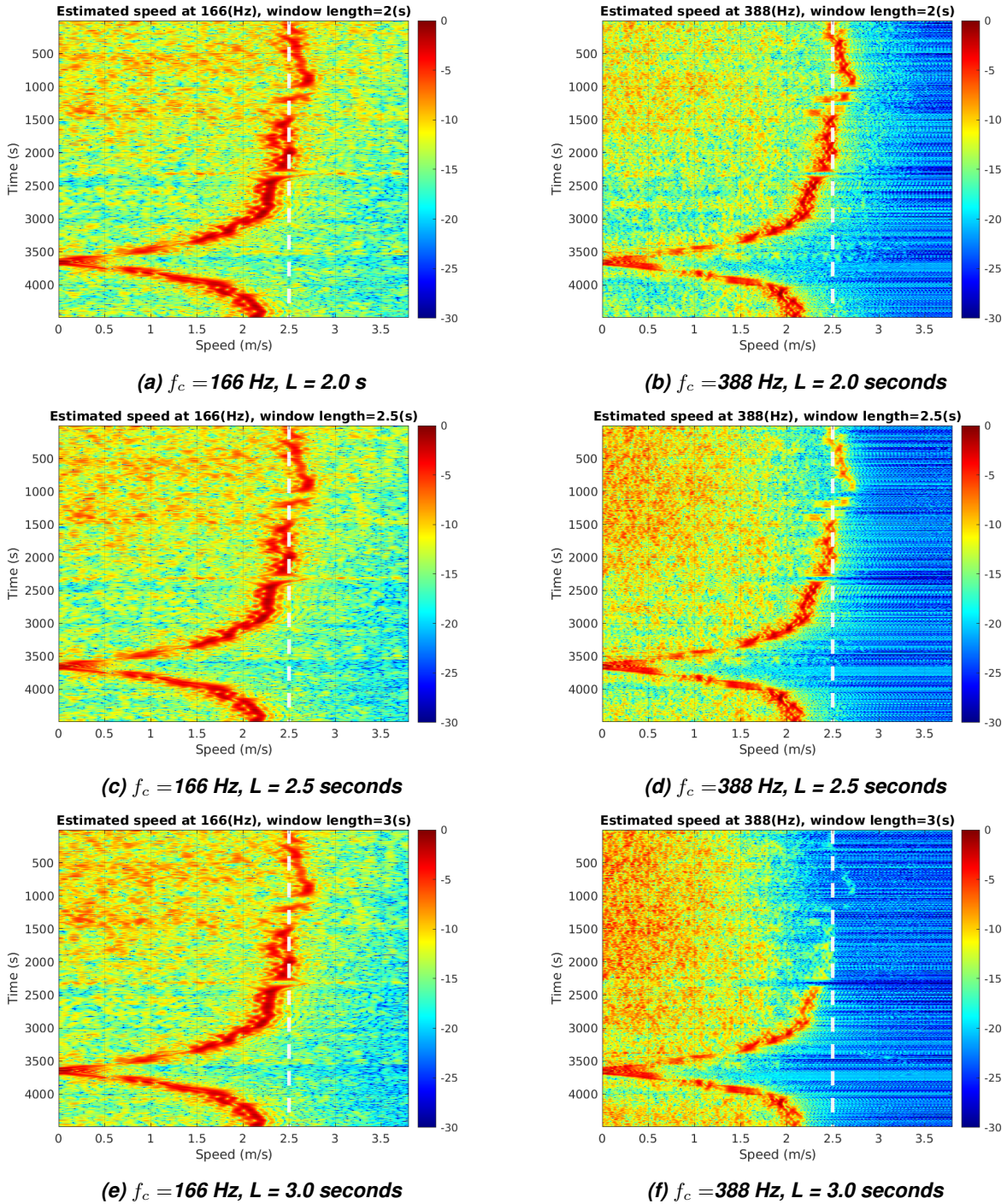


Figure 4: Effect of window length ( $L$ ) on the velocity estimation for different signal frequency ( $f_c$ ).

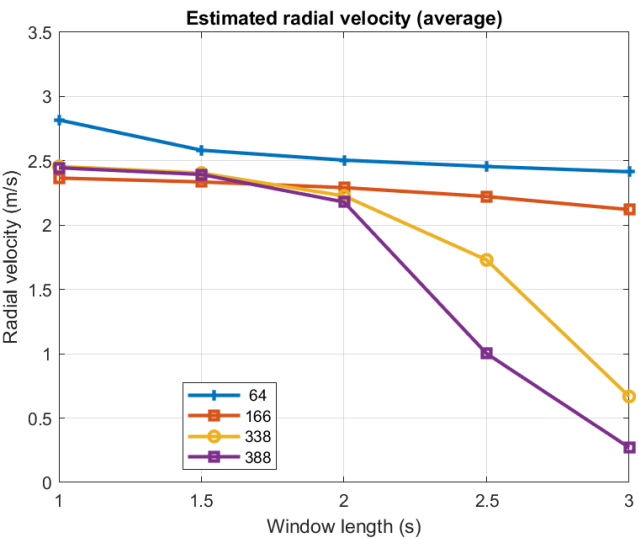


Figure 5: Average of the estimated velocity for the far distance condition (0 to 2400 seconds).

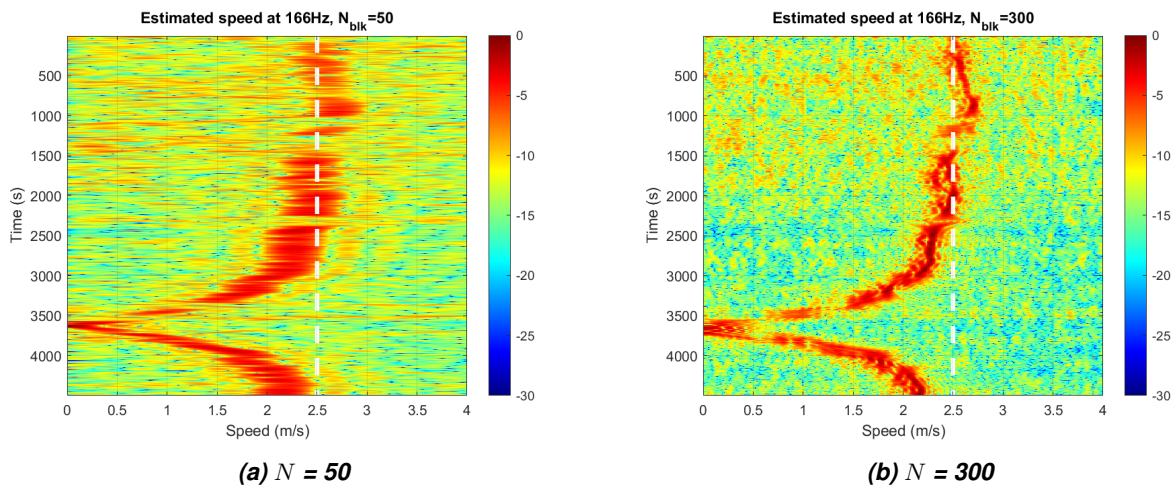


Figure 6: Effect of FFT length  $N$ .